Cholesterol Is Found To Reside in the Center of a Polyunsaturated Lipid Membrane

Thad A. Harroun,[‡] John Katsaras,[‡,§] and Stephen R. Wassall*[,||]

Department of Physics, Brock University, St. Catharines, Ontario L2S 3A1, Canada, Canadian Neutron Beam Centre, National Research Council, Chalk River, Ontario K0J 1J0, Canada, Guelph-Waterloo Physics Institute and Biophysics Interdepartmental Group, University of Guelph, Guelph, Ontario N1G 2W1, Canada, and Department of Physics, Indiana University-Purdue University Indianapolis, Indianapolis, Indiana 46202-3273

Received January 22, 2008; Revised Manuscript Received May 7, 2008

ABSTRACT: Previously, we reported neutron diffraction studies on the depth of cholesterol in phosphatidylcholine (PC) bilayers with varying amounts of acyl chain unsaturation [Harroun, T. A., et al. (2006) *Biochemistry 45*, 1227−1233]. The center of mass of the 2,2,3,4,4,6-D_6 deuterated sites on the sterol label was found to reside 16 Å from the middle of the bilayer in 1-palmitoyl-2-oleoylphosphatidylcholine (16:0-18:1PC), 1,2-dioleoylphosphatidylcholine (18:1-18:1PC), and 1-stearoyl-2-arachidonylphosphatidylcholine (18:0-20:4PC). This location places cholesterol's hydroxyl group close to the membrane surface, indicative of the molecule in its commonly understood "upright" orientation. However, for dipolyunsaturated 20:4-20:4PC membranes the label, thus the hydroxyl group, was found sequestered in the center of the bilayer. We attributed the change in location to the high level of disorder of polyunsaturated fatty acids (PUFA) that is incompatible with proximity to the rigid steroid moiety in its usual upright orientation. From that study, the unresolved question was whether the molecule was inverted or lying flat with respect to the membrane plane, in the middle of the bilayer. We have followed up those results with additional neutron experiments employing [25,26,26,26,27,27-D_7]cholesterol, a deuterated analogue labeled in the tail. These diffraction measurements unequivocally show cholesterol lies flat in the middle of 20:4-20:4PC bilayers.

Polyunsaturated fatty acids (PUFA)[1] constitute a biologically influential group of molecules whose physiological importance is becoming well established (*1*). High levels, sometimes exceeding 50 mol %, are found in the phospholipids of specialized membranes where their depletion impairs function (*2*). Neural membranes that accumulate phospholipids enriched in arachidonic (20:4) and docosahexaenoic (22:6) acids are the chief example. In retinal membranes, for instance, PUFA are particularly abundant, and nearly 30% of phosphatidylcholines (PCs) isolated from bovine rod outer segments are dipolyunsaturated (*3*). A multitude of disease states and chronic conditions are alleviated by dietary consumption of PUFA that elevates the modest concentration, usually less than 10 mol %, of PUFA-containing phospholipids in the plasma membrane (*1*). While interest in the topic has centered on the omega-3 class of PUFA lipids, it has also spanned a variety of human health issues, including PUFA-associated effects on protein signaling in inflammation and cancer (*4*), arteriosclerosis (*5*), and suppressive effects on the immune system (*6*). The efficacy of PUFA has been attributed to the formation of membrane domains enriched in PUFA-containing phospholipids (*2, 6–10*). According to this model, the high level of disorder of PUFA provides a local environment necessary for protein function.

Cholesterol is an essential component of mammalian cells and is either obtained from foods of animal origin (e.g., milk, cheese, meat, eggs, etc.) or synthesized in the endoplasmic reticulum (*11*). It is required for building and maintaining cell membranes, regulates their fluidity, and may act as an antioxidant (*12*). Recently, cholesterol has also been implicated in cell signaling processes, where researchers have suggested that it forms lipid rafts in the plasma membrane (*13, 14*), and has also been found to reduce the permeability of the plasma membrane to sodium and hydrogen ions (*15*).

Aside from cholesterol's many physiological roles, what is also becoming clear is its poor affinity for lipids containing unsaturation as opposed to saturated lipids that can more readily form domains with a higher level of conformational order (*16–20*). This unequal affinity for cholesterol has also been implicated in sorting different lipid species into membrane domains (*21*). Lipid rafts that serve as the platform for signaling proteins in the plasma membrane have received the most attention over the past decade (*22–24*). They are liquid ordered (lo) regions enriched in cholesterol and sphingolipids that possess predominantly saturated fatty acid (SFA) chains for which the sterol has high affinity. On the other hand, liquid disordered (ld) domains enriched in polyunsaturated phospholipids from which cholesterol is excluded by its aversion for PUFA, represent the opposite extreme that is much less well understood (*6, 9, 10*). To elucidate the details of the molecular interactions of cholesterol with PUFA, we have looked at the effect of polyun-

* To whom correspondence should be addressed: Department of Physics, Indiana University-Purdue University Indianapolis, Indianapolis, IN 46202-3273. Phone: (317) 274-6908. Fax: (317) 274-2393. E-mail: swassall@iupui.edu.

[‡] Brock University.

[§] National Research Council and University of Guelph.

[||] Indiana University-Purdue University Indianapolis.

[1] Abbreviations: PC, phosphatidylcholine; PUFA, polyunsaturated fatty acid(s); SFA, saturated fatty acids; SLD, scattering length density.

10.1021/bi800123b CCC: $40.75
Published on Web 06/11/2008

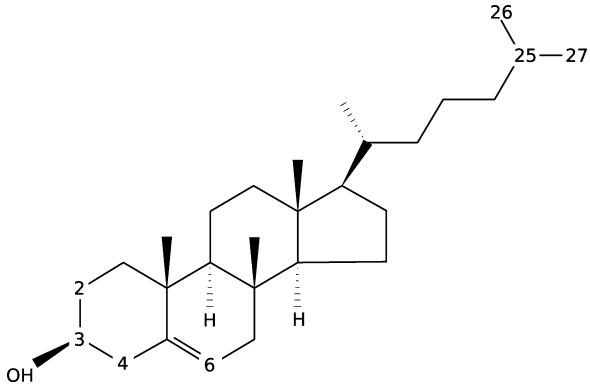

FIGURE 1: Deuterium label positions of cholesterol. The previous study involved the 2,2,3,4,4,6-D_6 hydrogen near the hydroxyl group on the steroid moiety, while the current study uses a 25,26,26,26,27,27,27-D_7 acyl tail label.

saturation on the depth to which cholesterol penetrates the membrane (*25*).

In our study, we used neutron diffraction to locate the depth of cholesterol's hydroxyl group in model membranes with varying amounts of acyl chain unsaturation. With selective deuterium labeling of the 2,2,3,4,4,6-D_6 hydrogen near the hydroxyl group on the steroid moiety (Figure 1), and neutron crystallographic techniques, it was possible to locate the center of mass of the label within the membrane directly, and unambiguously. In bilayers composed of PC molecules with a saturated acyl chain at the sn-1 position, or a monounsaturated acyl chain at both the sn-1 and sn-2 positions, the "top" of the steroid moiety resides 16 ± 1 Å from the bilayer center. This value corresponds to the location previously measured for cholesterol in its widely understood "upright" orientation in which the hydroxyl group sits near the aqueous interface, while the short hydrophobic tail extends toward the middle of the bilayer (*26*). However, in a dipolyunsaturated 20:4-20:4PC bilayer, when the entire hydrocarbon matrix consists of PUFA chains, our measurements indicate that the cholesterol steroid structure relocates to the center of the bilayer.

In this follow-up study, we resolve the remaining question of whether the change in cholesterol's organization in 20:4-20:4PC involves the molecule inverting, or a sequestration to the bilayer midplane. Using the same methods that were used previously, we used cholesterol with specific 25,26,26,26,27,27,27-D_7 deuterium labeling at the "bottom", or tail end, of the molecule (Figure 1). Together with the depth of the hydroxyl group, this information will establish the orientation of the long axis of the molecule with respect to the bilayer plane. Here we show that the tail of cholesterol resides at the center of the bilayer in both mono- and polyunsaturated PC lipids.

EXPERIMENTAL PROCEDURES

The methods of sample preparation and neutron diffraction follow exactly those described previously (*25*). PC lipids were purchased from Avanti Polar Lipids (Alabaster, AL) and tested for purity by TLC prior to use. The lipids studied were of the form 1,2-diacyl-*sn*-glycero-3-phosphatidylcholine, namely, dioleoyl (18:1-18:1PC) and diarachidonoyl (20:4-20:4PC). Sigma (St. Louis, MO) and CDN Isotopes (Pointe-Claire, QC) were the sources of unlabeled cholesterol and selectively deuterated [25,26,26,26,27,27,27-D_7]cholesterol, respectively.

All preparations of aligned multilayer samples were carried out in a helium-filled glovebox. Employing this precaution, necessary for the PUFA-containing phospholipids susceptible to peroxidation, reproducible results were obtained throughout data collection. Samples were checked for an absence of odor (a sensitive indicator of sample degradation) before and after data collection. During data collection, the repeat spacing was also monitored for gradual, irreversible changes. Sample purity, if suspect, was assessed for degradation by TLC to identify whether trace impurities (>1%) were present as would be implied by observation of more than a single spot. A total of 12 mg of phospholipid with 10 mol % cholesterol was codissolved in a chloroform/trifluoroethanol mixture (3:1). The solution was deposited on a silicon crystal substrate, and the solvent evaporated while the sample was gently rocked. The sample was then placed in a vacuum for ~2 h to remove traces of the solvent.

Neutron diffraction data were recorded at the Canadian Neutron Beam Centre's N5 beamline, located at the National Research Universal (NRU) reactor (Chalk River, ON), using 2.37 Å wavelength neutrons. The appropriate wavelength neutrons were selected by the (002) reflection of a pyrolytic graphite (PG) monochromator, while a PG filter was used to eliminate higher-order (i.e., $\lambda/2$, etc.) reflections. The samples were equilibrated, at room temperature, in a humid helium atmosphere for several hours and kept at 24.0 ± 0.5 °C during data collection. Samples were hydrated at fixed humidities using saturated salt solutions of KCl [84% relative humidity (RH)], KNO_3 (94% RH), and K_2SO_4 (97% RH) with 8 and 30 mol % D_2O.

Data correction and reconstruction of the bilayer profile proceeded as outlined previously (*25*). Briefly, the method takes the integrated area of the peak intensities for each order I_h and corrects for neutron absorption (C_{abs}), geometry of beam and sample widths (C_{flux}), and the Lorentz factor (C_{Lor}), resulting in the discrete structure factors $|F_h|^2 = C_{flux}C_{Lor}C_{abs}I_h$. The corrections are given by

$$C_{flux} = 1/\mathrm{erf}\left[\frac{L\sin(\theta)}{\sqrt{8}\sigma}\right] \quad (1)$$

$$C_{Lor} = \sin(2\theta) \quad (2)$$

$$C_{abs} = \alpha/(1 - e^{-\alpha}), \quad \alpha = \frac{2\mu t}{\sin(\theta)} \quad (3)$$

where μ is the absorption coefficient, t is the sample thickness, σ is the width of the beam, and L is the sample width. The absorption coefficient can be calculated alongside F_0, using the total neutron cross section (rather than just the coherent scattering cross section), the chemical composition (with 10% water by mass), and the assumption of a mass density of 1 g/cm ^{3}. The sample thickness can be estimated from the amount of material applied to a substrate of known area, and assuming an area per lipid of ~50 Å^2. All the corrections depend on the scattering vector $q = 4\pi\sin(\theta)/\lambda = 2\pi h/d$, where λ is the neutron wavelength, θ is the scattering angle, d is the unit cell size, and h is the Bragg order.

Although data were quantitatively similar to previous measurements, control samples of unlabeled cholesterol were again measured. This allows for slight differences in

Table 1: Measured Structure Factors for Membranes That Contain Deuterium-Labeled Cholesterol (B) and Protonated Cholesterol (A), under Different Hydration Conditions[a]

A

	18:1-18:1PC with 8% D_2O		20:4-20:4PC with 30% D_2O		20:4-20:4PC with 8% D_2O	
	F_h^D	δF_h	F_h^D	δF_h	F_h^D	δF_h
F_1	−2.599	0.082	−5.027	0.11	−2.356	0.09
F_2	−0.955	0.078	−0.824	0.09	−2.594	0.07
F_3	0.515	0.078	0.215	0.09	0.809	0.07
F_4	−0.278	0.078	0.096	0.09	0.0	0.0
F_5	−0.078	0.078	0.0	0.0	0.0	0.0

B

	18:1-18:1PC with 8% D_2O		20:4-20:4PC with 30% D_2O	
	F_h^D	δF_h	F_h^D	δF_h
F_1	−1.824	0.072	−4.192	0.09
F_2	−0.787	0.072	−0.327	0.07
F_3	0.535	0.072	0.280	0.07
F_4	−0.172	0.071	0.0	0.0
F_5	−0.060	0.071	0.0	0.0

[a] These structure factors were used in eq 5 to reconstruct the neutron scattering length density (SLD) profiles in Figures 3–5.

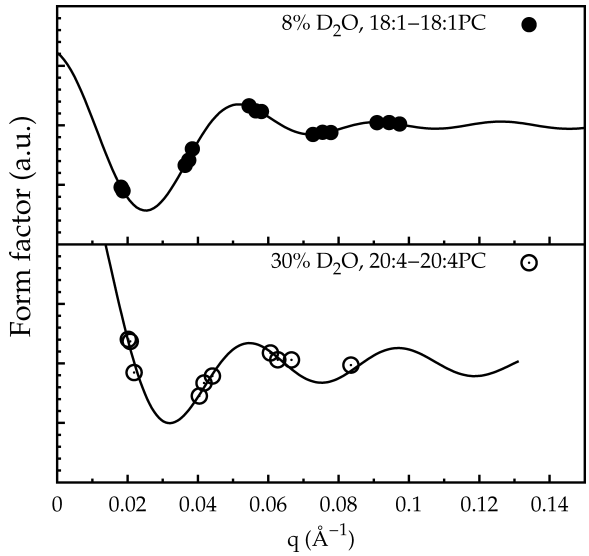

FIGURE 2: Demonstration of the phasing of structure factors of the unscaled data. For both cases, the unlabeled sample data are shown. The circles are the corrected but unscaled structure factors, and the solid line is the fit of eq 2 at the interpolated unit cell repeat spacing given in Table 2. At the three humidity values of 84, 94, and 97%, the 18:1-18:1PC repeat spacing was measured to be 51.2, 52.8, and 55.1 Å while the 20:4-20:4PC repeat spacing was 45.1, 46.3, and 48.5 Å, respectively.

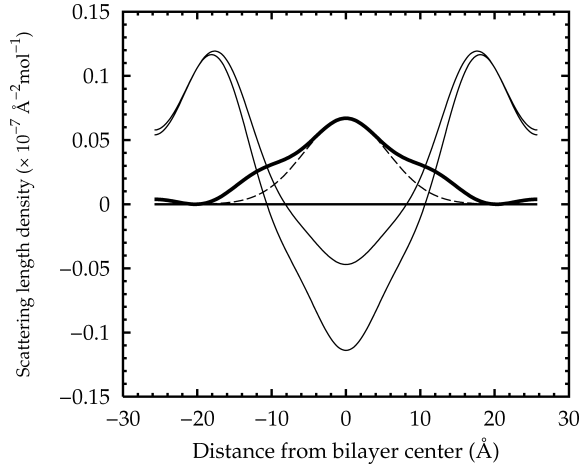

FIGURE 3: SLD difference profiles between labeled and unlabeled samples of 10 mol % cholesterol in 18:1-18:1PC. The origin of the abscissa is the center of the bilayer. The calculated SLD profiles have a spatial resolution h_{max}/d of ~10 Å and contain characteristic features. The negative dip at the center is from the terminal methyls, and the broad, positive peaks are due to the glycerol ester through phosphate regions. The bilayer thickness is defined as the distance between the maxima of the two peaks ($\chi^2 = 0.84$).

instrumental setup, which affect the resolution of the data and the width of the diffraction peaks. Typically, three to five individual structure factors (F_h) were measured, which appear in their final, corrected, and scaled form in Table 1, leading to a canonical resolution h_{max}/d of ~10 Å.

Data collected on the two labeled and unlabeled samples can be compared only after certain factors are taken into account. First, the unit cell size must be the same for the two samples. The amount of hydration is sensitive to slight variations in humidity, and although the RH was rigorously controlled by saturated salt solutions and temperature, variations in the measured unit cell size change due to random noise by ±0.2 Å (*27, 28*). This leads to small random errors in the measured structure factor amplitudes, especially for first- and second-order Bragg reflections, which can be minimized in the analysis in a couple of ways. First, one can measure the same sample with the same RH conditions, but different ratios of D_2O to H_2O. It has been shown that with this isotopic replacement method, each structure factor scales linearly as a function of D_2O concentration (*29*). From a straight line fit of the data, a new regularized structure factor can be obtained at a chosen D_2O concentration, effectively reducing noise by averaging across several measurements of the same sample. An additional advantage is increased confidence in the phasing of structure factors as odd and even values of the Bragg order peak h have opposite signs for the slope.

An alternative method, and the one used for this experiment, is to take several measurements at 8% D_2O (null neutron SLD), under different RH conditions (*30*). Despite the change in unit cell size, as water enters and exits the interbilayer spaces no SLD is being added or removed. Furthermore, across the range of RHs we are measuring, we assume only small, adiabatic structural changes are occurring within the bilayer. Thus, all the measured structure factors,

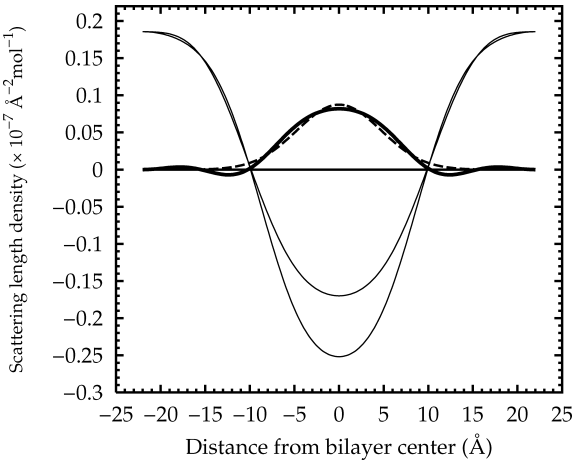

FIGURE 4: SLD difference profiles between labeled and unlabeled samples of 10 mol % cholesterol/20:4-20:4PC bilayers under 30% D_2O hydration conditions. The bilayer orientation is the same as in Figure 3. The broad peak at the center in gray is the measured distribution of the tail-labeled cholesterol, while the dashed curve is a fit with a single Gaussian function ($\chi^2 = 1.17$).

regardless of RH, can be fit to the same continuous form factor which is given by Shannon's theorem (*31*)

$$F(q) = \sum_{0}^{h_{max}} F_h \frac{\sin[\pi(qd-h)]}{\pi(qd-h)} \quad (4)$$

where F_h values are all of the measured structure factors. This method has the advantage of regularizing across all measurements of the same sample, simultaneously, and the determined continuous form factor is correct for any interpolated value of d. Phasing the structure factors can be accomplished as the continuous form factor of eq 4 must vary in a smooth, oscillatory way with hydration. Incorrect phase assignments are clear with inspection as an irregular change in the oscillations of the full form factor $F(q)$ (*30, 31*). Results of fitting eq 4 to the corrected but unscaled data at the various measured hydration levels are shown in Figure 2.

The neutron SLD profile $\rho(z)$ for a given sample can be constructed with the Fourier transform of the structure factors as follows:

$$\rho(z) = F_0 + \frac{2}{d}\sum_{h=1}^{h_{max}} F_h \cos(2\pi z h/d) \quad (5)$$

where z is the distance along the bilayer normal and F_0 is the calculated SLD of the entire unit cell per mole of sample, given in units of $Å^{-2}$ mol^{-1}. We find that placing the data on a SLD per mole basis, rather than the more common per lipid basis, is easier, especially for situations in which there are three or more system components. The difference between labeled (A) and unlabeled (B) samples can also be calculated with eq 5 using the difference in the structure factors:

$$F_h = F_h^A - F_h^B \quad (6)$$

as long as the structure factors for the labeled and unlabeled experiments can be placed on the same relative scale. Ideally, both data sets would be placed on the absolute scale of SLD, by multiplying the unscaled measured structure factors, F_h^A, by an experimental constant k^A that takes into account the experimental conditions. The scaled structure factors used in eq 6 are then given by

$$F_h^A = k^A F_h^{A*} \quad (7)$$

However, the unknown experimental constant k also depends on the amount of sample in the beam and, thus, is different for the labeled and unlabeled samples.

Table 2: Measured and Calculated Structural Parameters for [25,26,26,26,27,27,27-D_7]Cholesterol[a]

	18:1-18:1PC	20:4-20:4PC
repeat spacing (Å)	51.5	46.2
bilayer thickness (Å)	35.2	28.2
25,26,26,26,27,27,27-D_7 label depth (Å)	0.0 ± 0.0	0.0±0.0
25,26,26,26,27,27,27-D_7 label width (Å)	7.8 ± 0.6	6.6±0.3
2,2,3,4,4,6-D_6 label depth (Å)[b]	16.4 ± 0.3	0.0±0.0
2,2,3,4,4,6-D_6 label width (Å)[b]	4.2 ± 0.2	6.5±0.3
water layer Gaussian width (Å)	not available	6.3±0.6
water layer Gaussian center (Å)	not available	19.9±0.3

[a] The bilayer thickness is defined as the peak-to-peak distance of the bilayer SLD profiles shown in Figure 3. The center and width of the label locations are determined from the Gaussian peak fits to the difference SLD profiles such as shown in Figure 3. The results of the previous study with [2,2,3,4,4,6-D_6]cholesterol are included for completeness. The values listed here, and shown in subsequent figures for 18:0-18:0PC are for 84% RH conditions, and 20:4-20:4PC are for 94% RH conditions. [b] From ref (*25*).

Strategies for scaling the independent measurements of two samples whose only expected difference in SLD is through isomorphous replacement have recently been discussed by Han et al. (*28*). The method used here, and in the previous experiment, is similar in every regard to those methods. First, we expect that the SLD distribution of the label to be described by a Gaussian function centered at Z, of 1/e width σ and of SLD area A. The calculated structure factors for the label distribution only are then given by

$$F_h = 2Ae^{-(\pi\sigma h/d)^2}\cos(2\pi hZ/d) \quad (8)$$

To scale A to B, we use a point far from where we believe the label to be, z', and insist that the SLD profiles overlap in this region; $\rho^{A*}(z') = \rho^{B*}(z')$. The experimental constant k^A then scales A to B in such a way that simultaneously minimizes the difference between the measured (eq 6) and calculated structure factors (eq 8). We can further set the value of the label area A to be equal to $(F_0^A - F_0^B)d \approx 0.4 \times 10^{-7} \times d$ $Å^{-1}$ mol^{-1}. This number is determined with the expected isotopic compositions of the labeled and unlabeled samples, and using the neutron scattering length of -3.741×10^{-15} m for ^1H and $+6.671 \times 10^{-15}$ m for ^2H. The neutron scatting length is a measure of the nuclear force interaction of the neutron and the atom's nucleus and is related to the scattered amplitude of the neutron wave. This further puts both data sets into a "true" absolute scale, with the guarantee that

$$\int_0^d \rho(z)\,dz = F_0 d \quad (9)$$

If we pick z' wrongly, the scaling will not work; either the difference SLD profile will not show any kind of Gaussian-like peak, or there will be negative scaling factors. This is the situation encountered by Han et al. (*28*) with some of their data. Our encounter with this phenomenon will be discussed below. It should be pointed out that this method works very well on the "control" data of 18:1-18:1PC, where

the location of cholesterol is well-known, and which serves as a self-consistent, internal check.

RESULTS AND DISCUSSION

Figure 3 shows the scattering length density (SLD) profiles of 18:1-18:1PC containing 10 mol % unlabeled cholesterol or [25,26,26,26,27,27,27-D_7]cholesterol. The light curve with a maximum at the center is the difference in SLD between these two samples, while the dashed curve is a fit of a single Gaussian function to this peak. The full SLD profile of the sample with unlabeled cholesterol corresponds extremely well with the previously published data of Harroun et al. (*25*).

The origin of the abscissa is the centro-symmetric center of the unit cell, corresponding to the center of the bilayer, while the interlamellar water is found at the edges of the unit cell. The maxima in the SLD correspond to the combined glycerol ester and phosphate regions of the lipid bilayer and are very similar in both the labeled and unlabeled cholesterol membranes. Values for the bilayer hydrophobic thickness, defined by the distance between these peaks, are presented in Table 2. The negative dip in SLD, located at the bilayer center, is due to the disordered terminal methyl groups of the acyl chains. The curves differ the most in this region, where the curve representing the deuterium-labeled cholesterol has a higher, less negative value. This difference curve represents the distribution of hydrogen on the terminal methyls of the cholesterol.

At the edges of the unit cell, the SLD does not go strictly to zero, as might be expected for null scattering water. In fact, swelling experiments with 18:1-18:1PC using 0 and 8% D_2O have shown that the SLD at the unit cell edges can have significant positive values (*30*). The penetration of the choline into this region is substantial, and it is unlikely there will be any region that is lipid-free, bulk water.

The distribution appears to consist of two peaks, a central peak located at $z = 0$ Å and a pair of smaller satellite peaks at $z \approx \pm 10$ Å. It is debatable whether the outer peaks are real, corresponding to a second distribution of the cholesterol's deuterium label, or an artifact of a truncation error in the Fourier series. Such systematic errors can also be seen in the previous experiment, as shown in Figure 3 of Harroun et al. (*25*). Subtraction of the SLD curves is performed in reciprocal space, and a large number of structure factors (large h_{max}) in eq 5 is required to accurately represent a smooth Gaussian distribution function in real space, much more than is typically measured. This leads to a truncation in the Fourier series which manifests itself in undulations around the central peak of the distribution, like what was seen and discussed recently by Ruettinger et al. (*32*). Thus when we fit a Gaussian distribution function to the difference profile, since fitting is also performed in reciprocal space directly on the measured structure factors (*33, 34*), we focus on only the central peak. It should be pointed out that the peak area of the difference curve (Figure 3) appears much larger than the reported values shown in Table 2. The reason is the unit cell's mirror symmetry, where atoms in one half of the unit cell are reflected across the center (and edges) of the unit cell. Therefore, atoms, or groups of atoms, represented by distribution functions close to the center (or near the edges) of the unit cell are amplified by their mirror conjugates. With this in mind, we placed the data on an absolute scale requiring the proper area of the difference SLD profile be equal to the scattering length of the label, as mentioned above.

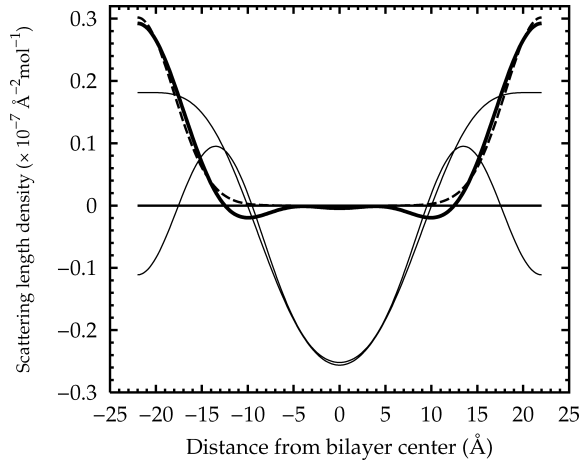

FIGURE 5: SLD difference profiles between unlabeled samples of 10 mol % cholesterol in 20:4-20:4PC under 8 and 30% D_2O hydration conditions. The bilayer orientation is the same as in Figure 3. The gray line is the measured interbilayer water profile, and the dashed line is a fit with a single Gaussian function. Fitting is performed in reciprocal space by taking the difference in the measured structure factors.

In the case of 20:4-20:4PC, due to time and sample constraints, it was not possible to obtain data for the labeled cholesterol under all 8% D_2O conditions. Nevertheless, we did acquire good data for 30% D_2O labeled and unlabeled samples, as well as 8% D_2O conditions for the unlabeled sample. With these data, we can still determine the label distribution from the difference in the 30% D_2O data. We explain this because such data, shown in Figure 4, are largely featureless and interpretation of the SLD curve is less obvious. It is often preferable to present data taken under 8% D_2O conditions, since the entire SLD curve is due to bilayer structure, only, and the contribution to the scattering from interlamellar water has been removed.

Figure 5 shows the data for 20:4-20:4PC with 10 mol % unlabeled cholesterol, under 8 and 30% D_2O conditions. Again, the light curve, with maxima at the unit cell edges and a value of $\approx$0 at the center, is the difference between the two sample conditions, while the dashed curve is the fit of a single Gaussian function. The 30% D_2O curve is dominated by the SLD of the water near the edges of the unit cell, whereas the 8% data are quantitatively similar to those depicted in Figure 2 of Harroun et al. (*25*). The hydrophobic core of the bilayer, since it excludes practically all water, is the same in both cases. Thus, when the curves are matched together and subtracted, the result is the distribution of interlamellar water in the unit cell.

After all of the 20:4-20:4PC data (Figures 4 and 5) were placed on an absolute scale according to the SLD area of the cholesterol label, the SLD area of the water distribution was fit and found to be $\approx 1.5 \times 10^{-7} \times d$ Å^{-2} mol^{-1}. If we assume that the water mass is $\sim$10% of the total sample mass, a reasonable assumption for 94% relative humidity, then we calculate that the difference in total SLD of the sample between 30 and 8% D_2O should be $1.7 \times 10^{-7} \times d$ Å^{-2} mol^{-1}, in good agreement with the measured value and good evidence that the scaling has been properly performed.

The width and center of the Gaussian fit to the water distribution are included in Table 2.

Figure 4 shows data for 20:4-20:4PC bilayers with 10 mol % labeled and unlabeled cholesterol, both hydrated with 30% D_2O. As with 18:1-18:1PC, the match in the lipid headgroup and water region is good, with the biggest difference being the bilayer center. The light curve centered at the origin is the difference profile. The distribution is described well by a single Gaussian function, while undulations, due to truncating an infinite Fourier series (eq 5), are also seen.

Thus, for both 18:1-18:1PC and 20:4-20:4PC, the tail of cholesterol is found to be in the center of the bilayer. When combined with the previously published data of Harroun et al. (*25*), we can reasonably deduce cholesterol's orientation in each bilayer. In 18:1-18:1PC, cholesterol is upright in its canonical orientation, with its hydroxyl group at the water−lipid interface and its acyl tail at the bilayer center. In the case of 20:4-20:4PC, where a single peak at the middle of the bilayer is seen with headgroup- and tail-labeled sterol, the molecule lies parallel to the plane of the bilayer sequestered between leaflets within the lipid matrix.

Cholesterol's reorganization in the dipolyunsaturated membrane is accompanied by a change in molecular mobilization. The width of the label distributions in Figures 3 and 4 represents the time- and sample-averaged fluctuation amplitude of the label in the direction normal to the bilayer plane. Thus, a gross picture of the overall mobility of cholesterol can be understood from the distribution widths. For the normal, upright cholesterol orientation in 18:1-18:1PC, we find that the hydroxyl headgroup of cholesterol is motionally constrained to an ~4 Å region at the water−lipid interface (*25*), while the disordered tail is freer to explore a larger (~8 Å) region (Figure 3). Thus, the overall depth of cholesterol in 18:1-18:1PC bilayers is fairly restrained. The comparative freedom of the tail is expected, since it resides in a much more flexible region of the membrane.

For 20:4-20:4PC, the entire sterol is now solvated at the same depth in the lipid acyl chain matrix. Thus, we find that both the headgroup (results from ref *25*) and tail (results shown in Figure 4) experience a 6.5−6.6 Å range of motion. Since all of the molecule finds itself in a single environment, it is likely that the label distributions represent whole body motion. What cannot be determined from the neutron scattering data is whether cholesterol undergoes much axial rotation or whether the plane of the flat steroid ring is coplanar with the bilayer plane. The answer is found in our previously reported D NMR spectra for [3α-D_1]cholesterol incorporated into 20:4-20:4PC (*16, 18*). Those spectra are powder patterns characterized by two intense peaks split by $\Delta\nu_r = 37$ kHz, symptomatic of anisotropic reorientation that is fast on the D NMR time scale (~10^{-6} s). The alignment of the molecule cannot be ascertained from the NMR data because the samples were aqueous multilamellar dispersions composed of bilayers randomly distributed in orientation relative to the magnetic field. All of these data are shown schematically in Figure 6.

We have hypothesized that aversion of cholesterol to PUFA promotes the formation of domains rich in polyunsaturated phospholipids from which the sterol is depleted and the segregation of the sterol into raftlike domains enriched with saturated sphingolipids (*9, 35, 36*). Support for this hypothesis has come from solid state NMR, DSC,

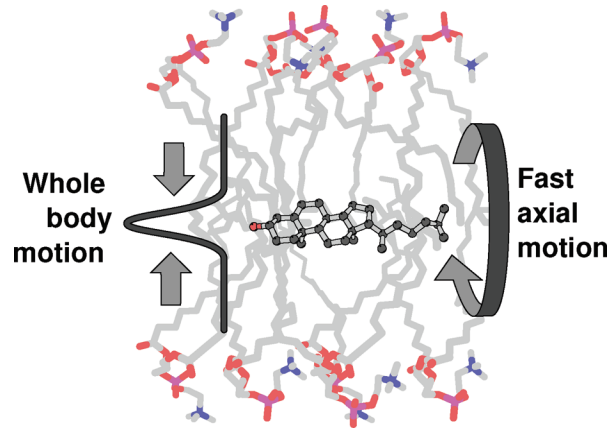

FIGURE 6: Schematic depiction of the location of cholesterol in 20:4-20:4PC membranes. The molecule is found by neutron diffraction to reside at the center of the bilayer and to be motionally constrained to ±6 Å of whole body motion. At the same time, the molecule also undergoes fast axial rotation, as determined by D NMR spectra.

and detergent extraction experiments. The findings from the neutron diffraction work reported here suggest that the poor affinity for PUFA may affect the transmembrane, as well as the lateral, distribution of cholesterol. A tendency to sit at the center of the PUFA-containing membranes, tipped over from the usual orientation where the hydroxyl group of the steroid moiety is anchored at the aqueous interface, would facilitate the flip-flop of sterol from one side of a membrane to the other. Indeed, enhanced rates of flip-flop were observed for cholesterol in recently published coarse-grained simulations that identified the presence of the sterol embedded between monolayers of arachidonic acid-containing PC bilayers (*37*). In plasma membranes, sphingolipids are primarily located in the outer monolayer (*23*), whereas PUFA are preferentially incorporated into phospholipids, such as phosphatidylethanolamine, that are more abundant in the inner leaflet (*38*). Thus, the presence of PUFA in the inner leaflet would enhance the transfer of cholesterol to the outer layer, potentially modifying raft composition and function. Consistent with this scenario, the accumulation of PUFA into plasma membranes was seen to result in a substantial redistribution of cholesterol to the outer leaflet (*39*).

In conclusion, we have completed a series of experiments that shows cholesterol lies flat in the midplane of 20:4-20:4PC bilayers. This remarkable change in the orientation of the sterol molecule in bilayers made up entirely of polyunsaturated acyl chains represents a dramatic manifestation of the high level of disorder possessed by PUFA. A reduced energy barrier to isomerization about the single bonds that separate the multiple double bonds in the recurring ═CH-CH_2-CH═ motif produces a rapidly fluctuating conformation (*40, 41*) that is incompatible with close approach to the rigid steroid moiety. To fully understand the interaction of PUFA with cholesterol, additional factors such as the location and number of double bonds in the polyunsaturated chain must be considered. They will be the subject of future experiments.

REFERENCES

1. Stillwell, W., and Wassall, S. R. (2003) Docosahexaenoic acid: Membrane properties of a unique fatty acid. *Chem. Phys. Lipids 126*, 1–27.
2. Salem, N., Jr., Kim, H. Y., and Yergey, J. A. (1986) in *Health Effects of Polyunsaturated Fatty Acids in Seafoods* (Simopoulos,

A. P., Kifer, R. R., and Martin, R. E., Eds.) pp 263−317, Academic Press, New York.
3. Aveldano, M. I. (1989) Dipolyunsaturated species of retina phospholipids and their fatty acids. *Colloq. INSERM 195*, 87–96.
4. Siddiqui, R. A., Harvey, K. A., Zaloga, G. P., and Stillwell, W. (2007) Modulation of Lipid Rafts by Omega-3 Fatty Acids in Inflammation and Cancer: Implications for Use of Lipids During Nutrition Support. *Nutr. Clin. Pract. 22*, 74–88.
5. Kratz, M. (2005) Atherosclerosis: Diet and Drugs. In *Handbook of Experimental Pharmacology* (von Eckardstein, A., Ed.) Vol. 170, pp 195−214, Springer, New York.
6. Shaikh, S. R., and Edidin, M. (2006) Polyunsaturated fatty acids, membrane organization, T cells, and antigen presentation. *Am. J. Clin. Nutr. 84*, 1277–1289.
7. Huster, D., Arnold, K., and Gawrisch, K. (1998) Influence of docosahexaenoic acid and cholesterol on lateral lipid organization in phospholipid mixtures. *Biochemistry 37*, 17299–17308.
8. Mitchell, D. C., and Litman, B. J. (1998) Effects of cholesterol on molecular order and dynamics in highly polyunsaturated phospholipid bilayers. *Biophys. J. 75*, 896–908.
9. Wassall, S. R., Brzustowicz, M. R., Shaikh, S. R., Cherezov, V., Caffery, M., and Stillwell, W. (2004) Order from disorder, corralling cholesterol with chaotic lipids. The role of polyunsaturated lipids in membrane raft formation. *Chem. Phys. Lipids 132*, 79–88.
10. Shaikh, S. R., and Edidin, M. A. (2006) Membranes are not just rafts. *Chem. Phys. Lipids 144*, 1–3.
11. Yeagle, P. L. (1993) in *Cholesterol in Membrane Models* (Finegold, L., Ed.) pp 1−12, CRC Press, Boca Raton, FL.
12. Smith, L. L. (1991) Another Cholesterol Hypothesis: Cholesterol as Antioxidant. *Free Radical Biol. Med. 11*, 47–61.
13. Papanikolaou, A., Papafotika, A., Murphy, C., Papamarcaki, T., Tsolas, O., Drab, M., Kurzchalia, T. V., Kasper, M., and Christoforidis, S. (2005) Cholesterol-dependent Lipid Assemblies Regulate the Activity of the Ecto-nucleotidase CD39. *J. Biol. Chem. 28*, 26406–26414.
14. Petrie, R. J., Schnetkamp, P. P. M., Patel, K. D., Awasthi-Kalia, M., and Deans, J. P. A. (2000) Transient Translocation of the B Cell Receptor and Src Homology 2 Domain-Containing Inositol Phosphatase to Lipid Rafts: Evidence Toward a Role in Calcium Regulation. *J. Immunol. 165*, 1220–1227.
15. Haines, T. H. (2001) Do Sterols Reduce Proton and Sodium Leaks Through Lipid Bilayers? *Prog. Lipid Res. 40*, 299–324.
16. Brzustowicz, M. R., Stillwell, W., and Wassall, S. R. (1999) Molecular organization of cholesterol in polyunsaturated phospholipid membranes: A solid state ^{2}H NMR investigation. *FEBS Lett. 451*, 197–202.
17. Niu, S. L., and Litman, B. J. (2002) Determination of membrane cholesterol partition coefficient using a lipid vesicle-cyclodextrin binary system: Effect of phospholipid acyl chain unsaturation and headgroup composition. *Biophys. J. 83*, 3408–3415.
18. Brzustowicz, M. R., Cherezov, V., Zerouga, M., Caffrey, M., Stillwell, W., and Wassall, S. R. (2002) Controlling membrane cholesterol content. A role for polyunsaturated (docosahexaenoate) phospholipids. *Biochemistry 41*, 12509–12519.
19. Brzustowicz, M. R., Cherezov, V., Caffrey, M., Stillwell, W., and Wassall, S. R. (2002) Molecular organization of cholesterol in polyunsaturated membranes: Microdomain formation. *Biophys. J. 82*, 285–298.
20. Pitman, M. C., Suits, F., MacKerell, A. D., Jr., and Feller, S. E. (2004) Molecular-level organization of saturated and polyunsaturated fatty acids in a phosphatidylcholine bilayer containing cholesterol. *Biochemistry 43*, 15318–15328.
21. Silvius, J. R. (2003) Role of cholesterol in lipid raft formation: Lessons from lipid model systems. *Biochim. Biophys. Acta 1610*, 174–183.
22. Simons, K., and Ikonen, E. (1997) Functional rafts in cell membranes. *Nature 387*, 569–572.
23. Brown, D. A., and London, E. (2000) Structure and Function of Sphingolipid- and Cholesterol-rich Membrane Rafts. *J. Biol. Chem. 275*, 17221–17224.
24. Pike, L. J. (2006) Rafts defined: A report on the Keystone symposium on lipid rafts and cell function. *J. Lipid Res. 47*, 1597–1598.
25. Harroun, T. A., Katsaras, J., and Wassall, S. R. (2006) Cholesterol Hydroxyl Group Is Found To Reside in the Center of a Polyunsaturated Lipid Membrane. *Biochemistry 45*, 1227–1233.
26. Léonard, A., Escriv, C., Laguerre, M., Pebay-Peyroula, E., Néri, W., Pott, T., Katsaras, J., and Dufourc, E. J. (2001) Location of Cholesterol in DMPC Membranes. A Comparative Study by Neutron Diffraction and Molecular Mechanics Simulation. *Langmuir 17*, 2019–2030.
27. Hristova, K., and White, S. H. (1998) Determination of Hydrocarbon Core Structure of Fluid Dioleoylphosphocholine (DOPC) Bilayers by X-Ray Diffraction Using Specific Bromination of the Double-Bonds: Effect of Hydration. *Biophys. J. 74*, 2419–2433.
28. Han, X., Hristova, K., and Wimley, W. C. (2008) Protein Folding in Membranes: Insights from Neutron Diffraction Studies of a Membrane β-Sheet Oligomer. *Biophys. J. 94*, 492–505.
29. Franks, N. (1976) Structural analysis of hydrated egg Lecithin and cholesterol bilayers I. X-ray diffraction. *J. Mol. Biol. 100*, 345–358.
30. Darkes, M. J. M., and Bradshaw, J. P. (2000) Real-time swelling-series method improves the accuracy of lamellar neutron-diffraction data. *Acta Crystallogr. D56*, 48–54.
31. Franks, N. P., and Lieb, W. R. (1979) The Structure of Lipd bilayers and the Effects of General Anaesthetics. *J. Mol. Biol. 133*, 469–500.
32. Ruettinger, A., Kiselev, M. A., Hauss, T., Dante, S., Balagurov, A. M., and Neubert, R. H. H. (2008) Fatty acid interdigitation in stratum corneum model membranes: A neutron diffraction study. *Eur. Biophys. J.* . (in press).
33. Wiener, M. C., and White, S. H. (1991) Fluid bilayer structure determination by the combined use of X-ray and neutron diffraction. I. Fluid bilayer models and the limits of resolution. *Biophys. J. 59*, 162–173.
34. Wiener, M. C., and White, S. H. (1991) Fluid bilayer structure determination by the combined use of X-ray and neutron diffraction. II. "Composition-space" refinement method. *Biophys. J. 59*, 174–185.
35. Shaikh, S. R., Dumaual, A. C., Castillo, A., LoCascio, D., Siddiqui, R. A., Stillwell, W., and Wassall, S. R. (2004) Oleic and docosahexaenoic acid differentially phase separate from lipid raft molecules: A comparative NMR, DSC, AFM, and detergent extraction study. *Biophys. J. 87*, 1752–1766.
36. Stillwell, W., Shaikh, S. R., Zerouga, M., Siddiqui, R., and Wassall, S. R. (2005) Docosahexaenoic acid affects cell signaling by altering lipid rafts. *Reprod. Nutr. Dev. 45*, 559–579.
37. Marrink, S. J., de Vries, A. H., Harroun, T. A., Katsaras, J., and Wassall, S. R. (2008) Cholesterol Shows Preference for the Interior of Polyunsaturated Lipid Membranes. *J. Am. Chem. Soc. 130*, 10–11.
38. Knapp, H. R., Hullin, F., and Salem, N., Jr. (1994) Asymmetric incorporation of dietary n-3 fatty acids into membrane aminophospholipids of human erythrocytes. *J. Lipid Res. 35*, 1283–1291.
39. Sweet, W. D., and Schroeder, F. (1988) Polyunsaturated fatty acids alter sterol transbilayer domains in LM fibroblast plasma membrane. *FEBS Lett. 229*, 188–192.
40. Feller, S. E., Gawrisch, K., and MacKerell, A. D., Jr. (2002) Polyunsaturated Fatty Acids in Lipid Bilayers: Intrinsic and Environmental Contributions to Their Unique Physical Properties. *J. Am. Chem. Soc. 124*, 318–326.
41. Huber, T., Rajamoorthi, K., Kurze, V. F., Beyer, K., and Brown, M. F. (2002) Structure of docosahexaenoic acid-containing phospholipid bilayers as studied by ^{2}H NMR and molecular dynamics simulations. *J. Am. Chem. Soc. 124*, 298–309.

BI800123B